ACCSCIENCE PUBLISHING

Materials Science in Additive Manufacturing

ORIGINAL RESEARCH ARTICLE

Anti-microbial plastic parts fabricated by high-speed sintering

Supplementary File

S1. Conventional and recent fabrication technologies to manufacture plastic articles

A method to fabricate anti-microbial plastics is to produce nanocomposites with anti-microbial nanoparticles[1]. Injection molding (IM) of plastics compounded with suitable nanoparticles (e.g., metals and metal oxides) is the common fabrication approach to manufacture nanocomposites. However, with contact biocides (requiring direct contact with the microbe) like $Mg(OH)_2$, IM will tend to embed the nanoparticles within the plastic, making them inactive (as demonstrated in this study). Additive manufacturing (AM) is emerging as a viable mass manufacturing method, specifically through powder bed fusion (PBF). This study presents a solution to manufacture freeform plastic articles with anti-microbial properties by coating them with biocidal nanoparticles using Powder Bed Fusion (PBF) technology.

S2. AM technologies

AM, also known as 3D printing, is a method of building an article layer-by-layer from a computer-aided design (CAD) model of the part. The CAD model is digitally sliced into layers of a specific thickness[2-4]. AM is currently used for manufacturing parts from polymers, metals, and ceramics. For plastics, AM complements IM, as it enables free-forming, that is, manufacturing parts without molds. This allows for the creation of intricate shapes, like lattice structures, that cannot be produced by any other method. However, the process of layer-by-layer building is inherently slow. AM was initially used for rapid prototyping but has now advanced to manufacturing functional parts.

Herein, we briefly discuss AM processes that are industrially scalable for polymers. PBF is a technology that utilizes polymer powder as raw material. Fused layer modeling (FLM) is another AM technology for making plastic parts from polymer filaments. PBF features faster manufacturing speeds than FLM, as multiple shapes (identical or different) can be built simultaneously on the powder bed. In contrast, an FLM machine requires a separate printing head for each part if printed concurrently, though it can produce large industrial parts.

All AM technologies have their respective advantages and disadvantages, suggesting that the more successful methods are likely to coexist with conventional fabrication methods. In the context of this work, PBF is more suitable for surface-embedding of contact biocides like $Mg(OH)_2$ platelets on the printed articles. FLM articles made with contact biocides are expected to be inert and behave like IM articles with little anti-microbial activity.

S3. Powder bed fusion (PBF)

PBF processes utilize electromagnetic radiation as the energy source to sinter/melt a pre-heated polymer powder in selected areas. For PBF, semi-crystalline polymers are more compatible than amorphous ones, and polyamide (PA) 12 is the most commonly used powder. The powder bed is held at a temperature within the sintering window, where the powder bed surface temperature ranges between the melting and recrystallization temperatures of the semi-crystalline polymer; it is transiently allowed to surpass its melting temperature in selected areas that correspond to the cross-section of the part. Consequently, this induces the polymer powder to melt (in the selected area) and subsequently solidify into a cohesive polymer layer on cooling. The powder bed is lowered, and a fresh layer of powder is added over the sintered layer. This layer-by-layer process is iterated across all cross-sections of the part until a fully realized 3D component is manufactured[2-12].

According to DIN ISO 52900, the two variants of PBF for polymers are classified as PBF with a laser beam (PBF-LB) and PBF with an infrared (IR) radiation lamp (PBF-IR). In the PBF-LB method, an IR laser beam (LB) (usually with a wavelength of 10.6 μm for a CO_2 laser) is used to melt the powder. A LB is characterized by a monochromatic beam of coherent radiation that is collimated. This allows the energy to be concentrated in an intense beam. PBF-LB was invented by Beaman and Deckard as a method to form complex plastic parts without molds, using a digital 3D model of the desired part[5]. It uses a polymer powder in a bed as feedstock. The IR laser rasters the cross-section of the part to fuse the polymer particles in the selected area. The PBF-LB AM process is also commonly known under the trade name of machine manufacturers as "selective laser sintering" (SLS)[2,3,5,6].

In the PBF-IR method, an incandescent IR lamp is used, which emits polychromatic, incoherent radiation (predominantly IR but also includes visible wavelengths) over the entire bed. The PBF-IR process combines the PBF method with the inkjet printing technology. The selective energy input is achieved using IR light-absorbing ink, usually carbon black ink, which is applied to the area corresponding to the part's cross-section by inkjet printing with piezo print heads. Thereafter, a traveling IR lamp moves across the entire area of the powder bed. The blackened powder areas on which the ink has been applied absorb more energy and are melted/sintered, whereas the areas of the bed where the ink was not applied remain in the powder phase. There are variants of the PBF-IR process, and they are also known under trade names such as High-Speed Sintering® (HSS) from the machine manufacturer voxeljet AG (Germany), Multi Jet Fusion® from the machine manufacturer HP Inc. (United States), and Selective Absorption Fusion® from machine manufacturer Stratasys Ltd. (United States). In this work, an HSS machine was used to manufacture polymer parts (disks and tensile bars) using PA 12 powder[12].

In the case of the PBF-LB (SLS) method, the production time per layer depends on the degree of utilization of the build volume (part volume to build volume) due to the local application of the IR energy. A larger part section will take longer to fuse with the laser than a small section. This dependency is eliminated in PBF-IR (HSS) due to the 2D energy input across the powder bed surface in a single pass of the IR lamp. Hence, in PBF-IR, there is a constant production time per layer. This is evident in the fact that PBF-LB requires one or two lasers to raster the surface of each part serially, whereas PBF-IR irradiates the entire bed in a single pass with a traveling IR lamp, making it a faster process. Therefore, the time to fuse the cross-sections of various parts in the powder via PBF-IR is shorter, suggesting that higher productivity can be achieved with PBF-IR (HSS) compared to PBF-LB (SLS), increasing its potential for industrial production. The area that can be fused per second can be compared: PBF-LS with one laser: 1750 mm^2/s; PBF-IR with one print head: 54600 mm^2/s. Thus, there is the possibility of scalability of the PBF-IR process by enlarging the build volume without decreasing the productivity. Another advantage of PBF-IR over PBF-LB (HSS over SLS) is that the energy is absorbed more gradually, while with the laser, the high intensity can burn and damage the polymer.

S4. HSS

The HSS process is schematically displayed in Figure S1 below.

Images of the HSS process from the manufacturing machine are also displayed in Figure S2. The process is illustrated for the fabrication of a tube from PA 12 powder. The printed cross-section resembles a ring. In this study, the articles (disks and tensile bars) can be considered 2 ½ dimensional. Hence, the printed cross-section does not change with building height; for example, for the disks, the inkjet-printed area is a circle of constant cross-section. It is emphasized that both PBF-LB and PBF-IR can produce 3D articles, where the cross-sectional areas change with height. In such cases, the areas scanned by the laser or inkjet-printed will change with height.

In this work, a VX200 HSS machine (voxeljet AG, Germany) was used for part manufacturing. As the part is a simple disk with a diameter of 2 cm, the ink jetted area is a circle with a 2 cm diameter.

In HSS, the first layer of the polymer powder is pre-heated on the build platform with an overhead lamp to a temperature a few degrees below the melting point of the polymer. The build chamber of the HSS machine, where the overhead lamp was located, contained six ceramic radiators to reach the selected process temperature and maintain a homogenous temperature distribution on the powder bed surface. The build box consisted of a floor plate that is vertically moveable and heatable, surrounded by four separately heatable walls [30]. The dimensions of the build box of the machine used for this work were 290, 140, and 180 mm in the x-, y-, and z-directions, respectively, which resulted in a maximum build volume of 7308 cm^3. The layer thickness is defined by the stroke of the floor plate in the negative z-direction. A traveling recoater with a vibrating blade system was used to add each layer of PA 12 powder. The powder output was determined by the recoater gap, the intensity of vibration, and the flow properties of the powder. The selective energy input is realized by the combination of IR radiation-absorbing material (RAM), which is selectively applied to the powder bed surface by a piezo print head and the traveling IR lamp[10]. The energy supplied by the traveling IR lamp melts the polymer powder RAM-covered areas, while the unprinted polymer powder does not melt and solidify (Figure S2).

S5. The inkjet printing module of the VX200 HSS machine

The ink-printing module, consisting of three XAAR 1003 print heads arranged staggered in two rows, was connected to the machine´s fluid circulation system. For manufacturing, the voxeljet AG HSS Ink Type B was used,

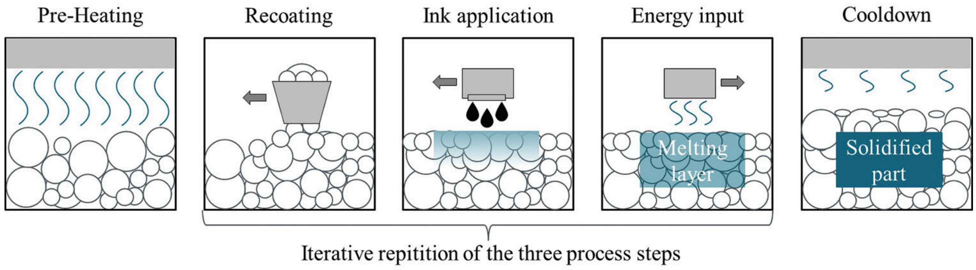

Figure S1. Schematic illustrating the High-Speed Sintering® process. Pre-heating: The powder bed is pre-heated to 10 – 20°C below the melting point of the polymer. Recoating: Application of a new monolayer of powder. Ink application: The cross-section of the part is inkjet-printed with radiation-absorbing ink. Energy input: A traveling infrared lamp traverses the bed and fuses the ink jetted area. The powder bed is lowered, and the process is repeated multiple times (recoating → ink application → energy input). Cool down: After the required number of iterations, the solidified part is removed from the powder after cooling

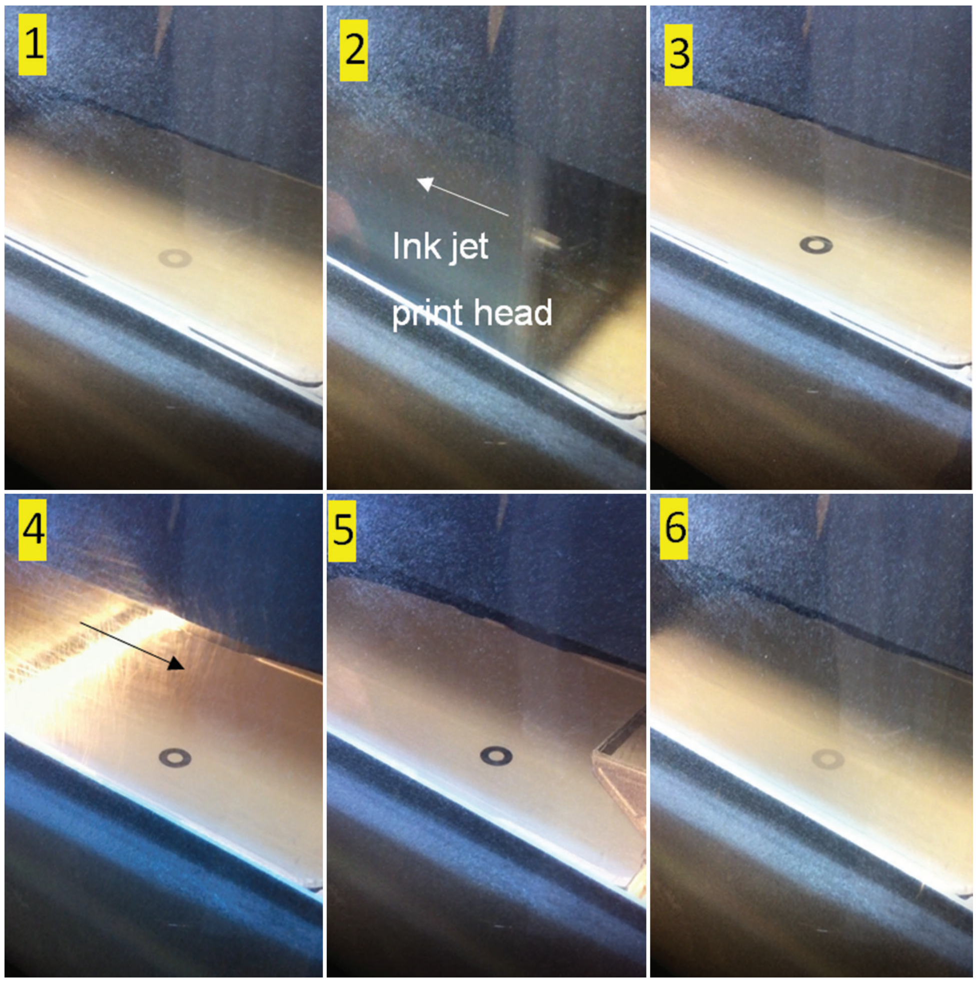

Figure S2. The high-speed sintering process for building a tube. (1) the PA 12 powder bed with a thin layer of powder deposited over the previously sintered layer (faint ring) is pre-heated with fixed overhead IR lamps to a few degrees below the melting point of the polymer. (2) The inkjet printer moves over the bed and prints the cross-section of the tube. (3) The black ring is left on the bed by the inkjet printer. (4) A traveling IR lamp moves across the bed, and the blackened area absorbs more heat than the surrounding white powder. (5) The polymer powder in the black region is fused in the plane and to the layer below. (6) is the same as (1); the powder recoater adds a new layer of PA 12 powder and the process repeats 2→3→4→5→6/1
Abbreviation: PA: Polyamide; IR: Infrared

containing carbon black. The VX200 HSS machine utilizes computer software to partition the CAD part into layers, a process known as slicing. Each layer generates a bitmap, delineating ink application positions and thereby defining part-geometry dimensions per layer. The standard 8-bit bitmap comprises precisely 256 gradations of gray, denoted as gray values (GV), ranging from 0 for black to 256 for white. Due to software limitations, the voxeljet VX200 HSS machine aggregates certain GV ranges into six distinct gray scales (GS). Equipped with the Xaar 1003 GS6 print head, the machine allows for droplet volume adjustment through 6 GV, incrementing by 6 pL from 0 to 36 pL/dot, at a resolution of 360 dots per inch (dpi). Consequently, each pixel and corresponding print droplet measures approximately 70 µm. A higher GS correlates with increased ink application, while a lower GS corresponds to reduced ink deposition. The traveling sintering lamp was equipped with a 3 kW halogen lamp to emit IR radiation. The selective energy input into the parts is determined by the combination of the travel speed across the powder bed, the power of the sintering lamp, and the amount of applied ink. The process was repeated until the part was built layer-by-layer. After the build, the build chamber was cooled down, and the parts were extracted and de-dusted (Figure S1).

S6. Test method for anti-microbial activity of the plastic nanocomposite

In anti-microbial testing, the anti-microbial activity of surfaces can vary according to the testing protocol. Multiple tests can assess a plastic's anti-microbial activity, including the "disk diffusion test." Bacteria are first cultured in an agar plate; the plastic containing the anti-microbial agent is placed in the center of the agar bacterial culture. If the anti-microbial agent is water soluble and effective, it will leach out, creating a visible inhibition zone around the disk where bacteria are killed. However, when this method was applied to plastic disks coated with $Mg(OH)_2$ nanoplatelets (NPs), no inhibition zones were observed – not because $Mg(OH)_2$ is ineffective, but because its anti-microbial mechanism does not rely on ion leaching.

In another test method, the plastic test disks (control and active) are placed in separate wells. Test bacteria are grown in a broth, and 0.1 mL droplets of the bacterial suspension are first added to the disks in the wells. After specific time intervals, 5 mL water is added to wash the wells, and the solution is transferred to agar plates for incubation. The bacterial colonies on the agar plates are counted. If the additive in the test disks does not have anti-microbial activity, it will exhibit bacterial growth similar to the control. Conversely, if the additive is effective in killing bacteria, there will be a decrease in the bacterial colony count. This test method is effective when bacterial killing is due to leached ions rather than bacterial interactions with the nanoparticles. It should also work in cases where direct contact between the anti-microbial agent and the bacterium is required. However, this method is static and does not prevent the build-up of a layer of dead bacteria on the surface. Another issue is that when bacterial media are added to the plastic sheet's surface as droplets, it may not spread evenly due to wetting problems, potentially leading to high variation in the testing data.

There is an ISO 22196 standard for testing bacteria on non-porous substrates, such as plastics (film covering technique), as well as ISO 21702 for testing viruses. A 50 × 50 mm sheet of the test plastic sheet is placed in a petri dish; 0.4 mL of the microbial inoculum is dropped on a 40 × 40 mm area of the plastic sheet. A thin cover film is then placed on the area with the liquid, and the petri dish is covered. After a specified period, the inoculum is washed and plated in agar, and the bacterial colony is counted. As there is no agitation in this method, the microbes can adhere to the test article, which may affect bacterial harvesting and counting. We did not adopt ISO 22196 in this study; our PA 12 parts made by HSS have a slightly porous quality, and the ISO test method is only applicable for non-porous substrates.

Hence, we devised the rotating chamber method with Aqua Resources Corp. (the USA) to address some of the limitations mentioned above. In this method, the bacteria are cultured in a broth; the test disks (control and sample expected to have anti-microbial activity) are placed in a plastic pod that can be closed and rotated in a machine. Contact lens pods from Bausch + Lomb (Germany) were adapted for holding the anti-microbial plastic disks, which were manufactured by HSS and IM with dimensions to fit the pods, allowing some spare volume for adding the bacterial broth. Rotation of the pods (Figure S3) ensured constant surface renewal with the broth. It also works

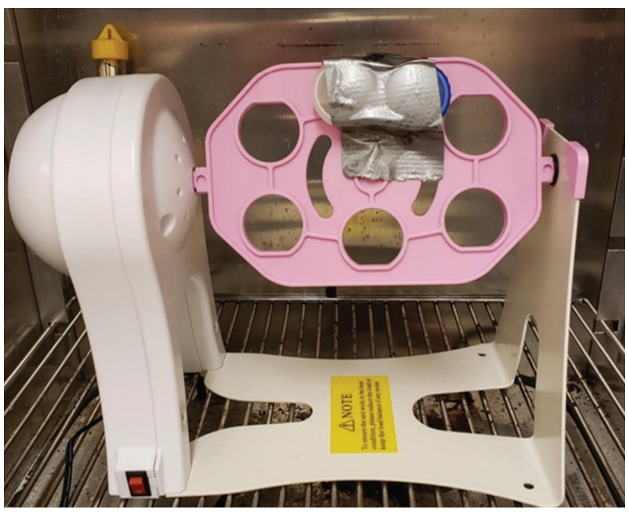

Figure S3. The pods were taped to the device for rotating them to prevent dead bacteria build-up on the surface of the polyamide 12 disks. The pink holder rotates around its central axis with disks without an ionic diffusion mechanism to kill the bacteria. For example, with $Mg(OH)_2$, which relies on contact killing, bacteria are killed through direct contact with NPs embedded on the surface of the plastic. The rotation of the pods ensures the dead bacteria do not accumulate and form a biofilm on the active surface. Thus, the active surface is continuously exposed to live bacteria in the broth. This method demonstrates good repeatability of the results and was employed in this study.

There is often uncertainty about whether the test method represents real-world situations. For example, a door handle made of anti-bacterial plastic may not undergo surface wiping to remove dead bacteria; instead, fresh living bacteria would be deposited over the biofilm of previous bacterial debris through repeated manual contact. Nevertheless, our rotating chamber method effectively demonstrates whether a plastic with an anti-microbial agent is active or inactive against microbes, relative to a non-active plastic and compared to a material like copper, which is known to be effective.

S7. Reactive oxygen species (ROS) and their anti-bacterial role

ROSs are highly reactive radicals formed from O_2, such as peroxides, superoxide, hydroxyl radical, singlet oxygen, and alpha-oxygen. Examples of ROS are $OH^•$, $O_2^{•-}$, $RO^·$, $RO_2^•$, $NO^·$ and NO_2.

Certain metal oxides such as TiO_2 and ZnO, when in nano size, can be excited by light and react with molecular oxygen to generate ROS, similar to ROS generation by $Mg(OH)_2$. However, Dong *et al.*[13] demonstrated that $Mg(OH)_2$ NPs can kill *Escherichia coli*, even in dark conditions; hence, photocatalytic ROS generation may not be involved in the anti-bacterial mechanism. Zhu *et al.*[14] displayed via immunofluorescence tests that $Mg(OH)_2$ induced macrophages (white blood cells that fight microbes) to generate ROS to kill microbes; this suggests that the mechanism is not due to ROS generated directly by the $Mg(OH)_2$ NPs, but rather ROS induced by $Mg(OH)_2$ NPs in the body's immune system.

References

1. Babutan I, Lucaci AD, Botiz I. Antimicrobial polymeric structures assembled on surfaces. *Polymers* (*Basel*). 2021;13:1552.

   doi: 10.3390/polym13101552

2. Schmid M. *Selektives Lasersintern (SLS) Mit Kunststoffen: Technologie, Prozesse und Werkstoffe*. Munich: Hanser; 2015.

3. Fahad M, Hopkinson N. Evaluation and comparison of geometrical accuracy of parts produced by sintering-based additive manufacturing processes. *Int J Adv Manuf Technol*. 2017;88:3389-3394.

   doi: 10.1007/s00170-016-9036-z

4. Hopkinson N, Hague R, Dickens P. *Rapid Manufacturing: An Industrial Revolution for a Digital Age*. Hoboken, New Jersey: Wiley-Blackwell; 2005.

5. Beaman JJ, Deckard CR. *Selective Laser Sintering with Assisted Powder Handling*. U.S. Patent 4,938,816A; 1986.

6. Bashir Z, Gu H, Yang L. Evaluation of poly(ethylene terephthalate) powder as a material for selective laser sintering, and characterization of printed part. *Polym Eng Sci*. 2018;58:1888-1900.

   doi: 10.1002/pen.24797

7. Hopkinson N, Erasenthiran P., ' Method and Apparatus for combining particulate material', US Patent 7,879,282 B2; 2011.

8. Ellis A. *Surface Topography: Metrology and properties*. Vol. 3. IOP Publishing Ltd.; 2015. p. 34005.

9. Brown R. 'Not Just Nylon… Improving the Range of Materials for High Speed Sintering. In: *Solid Freeform Fabrication Symposium*; 2018.

10. Pezold D, Wimmer M, Alfayez F, Bashir Z, Döpper F. Evaluation of polyethylene terephthalate powder in high speed sintering. *Polymers* (*Basel*). 2022;14:2095.

    doi: 10.3390/polym14102095

11. Ligon SC, Liska R, Stampfl J, Gurr M, Mülhaupt R. Polymers for 3D printing and customized additive manufacturing. *Chem Rev*. 2017;15:10212-10290.

    doi: 10.1021/acs.chemrev.7b00074

12. Hopkinson N, Smith PJ. Industrial 3D inkjet printing/additive manufacturing. In: *Handbook of Industrial Inkjet Printing: A Full System Approach*. United States: John Wiley and Sons; 2017. p. 649-660.

13. Dong C, Song D, Cairney J, Maddan OL, He G, Deng Y. Antibacterial study of Mg(OH)2 nanoplatelets. *Mater Res Bull*. 2011;46:576-582.

    doi: 10.1016/j.materresbull.2010.12.023

14. Zhu Y, Tang Y, Ruan Z, *et al*. Mg(OH)2 nanoparticles enhance the antibacterial activities of macrophages by activating the reactive oxygen species. *J Biomed Mater Res*. 2021;109:2369-2380.

    doi: 10.1002/jbm.a.37219